Proceedings of ASME IMECE:
2002 ASME International Mechanical Engineering Congress and Exposition
November 17-22, 2002, New Orleans, LA

IMECE2002-39370

SYNTHESIS AND CHARACTERIZATION OF METAL-CERAMIC THIN FILM NANOCOMPOSITES WITH IMPROVED MECHANICAL PROPERTIES

D. Kumar, N. Sudhir, S. Yarmolenko, Q. Wei, and J. Sankar
Center for Advanced Materials and Smart Structures
Department of Mechanical Engineering
North Carolina A & T State University, Greensboro, NC 27411

J. Narayan
Center for Advanced Materials and Smart Structures
Department of Materials Science and Engineering
North Carolina State University, Raleigh, NC 27695

S.J. Pennycook
Solid State Division
Oak Ridge National Laboratory, Oak Ridge, TN

ABSTRACT

Thin films composite materials consisting of metallic nanocrystals embedded in an insulator host have been synthesized using alternating-target pulsed laser deposition of Fe/Ni and Al_2O_3. The evaluation of structural quality of the thin film composites using high resolution transmission electron microscopy and scanning transmission electron microscopy with atomic number contrast has revealed the formation of a biphase system with thermodynamically driven segregation of Ni and alumina during pulsed laser deposition. The best hardness values of the thin film composites, measured using nanoindentation techniques, was found to 20-30% larger than pure alumina films fabricated under identical conditions. The improvement in values of hardness of Al_2O_3 thin films by embedding metal nanocrystals is related to the evolution of a microstructure which efficiently hinders the manipulation and movement of dislocation and the growth of microcracks, which in turn, is achieved by grain boundary hardening.

INTRODUCTION

Composite materials consisting of metallic clusters or crystals of nanometric dimension embedded in an insulator host exhibit special optical, electrical, magnetic, and mechanical properties which have opened many possibilities of their use in various technological applications [1-11]. For example, metal nanocrystals embedded in insulating materials offer enhanced mechanical properties, making them a promising candidate for use in machining tools [10-14]. The search for materials with enhanced hardness is driven by both the scientific curiosity of researchers to explore the possibilities of synthesizing a material whose hardness could approach or even exceed that of diamond and the technical importance of hard materials for wear protection of, e.g. machining tools. The importance of hard wear protective coatings for the machining applications is illustrated by the fact that today more than 40 % of all cutting tools are coated by wear resistant coatings and the market is growing fast. Wear resistant hard coatings for high speed dry machining would allow the industry to increase the productivity of expensive automated machines and to save on the high costs presently needed for environmentally hazardous coolant.

The metal nanocrystals embedded in insulating materials have been synthesized by quenching and heat treatments [15], sol-gel processes [16], sputtering [17], and ion implantation [18]. Most of these processes are multi-step processes, in which a post-deposition treatment is often needed to optimize the properties. However, these treatments can also alter the average grain size, size distribution, and spatial arrangement of the nanocrystals, with the possible unfavorable effects on the mechanical properties of the nanocomposites. Unlike these methods, multiple target sequential pulsed laser deposition (PLD) permits independent control of synthesis of the nanocrystals and the embedding matrix. PLD has shown particular success in stoichiometric thin film deposition of complex oxides. Energetic (>100 eV) ions produced by ablation yield smooth, high-density films with good adhesion, especially desirable for mechanical applications. In this paper we report the fabrication of alternating-target PLD of Fe and Ni

Copyright © 2002 by ASME

nanocrystals embedded in Al_2O_3 matrix. The nanocomposite exhibits superior mechanical properties with enhanced hardness and Young's modulus.

EXPERIMENTAL DETAILS

Nanocrystalline nickel and iron crystallites were embedded in alumina matrix using a KrF excimer laser (252 nm, 30 ns full width at half maximum) focused alternately onto high-purity targets of nickel or iron and alumina. The depositions were carried out on silicon substrates in a high vacuum environment (~5 X 10^{-7} Torr). The substrate temperature was approximately 500 ^{o}C. The energy density and repetition rate of the laser beam used were 2J/cm^2 and 10 Hz, respectively. The size distribution of metallic particles (Fig. 1) and the crystalline quality of both the matrix and metallic particles were investigated by cross-sectional scanning transmission electron microscopy with atomic number (Z) contrast (STEM-Z). Table 1 lists the hardness and particle size of nanocomposites produced using different metal deposition time.

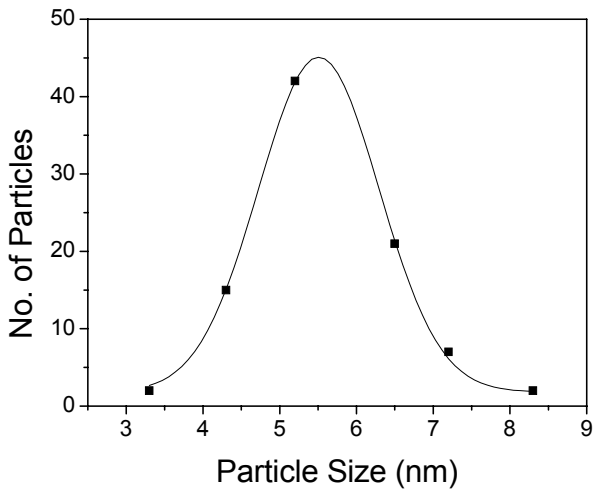

Figure 1. Size distribution of Ni particles in alumina matrix. The solid line is a log-normal fit to the data points.

Table 1. Hardness and particle size of nanocomposites produced using different metal deposition time.

Deposition Time (s)	Fe-Al_2O_3 system		Ni-Al_2O_3 system	
	Fe-size	Hardness (GPa)	Ni-size	Hardness (GPa)
20	3	15	4	27.0
40	4.5	20	6	23.5
60	7	28	8	24.2
80	9	16	10.5	24.0

RESULTS AND DISCUSSION

Shown in Fig. 2 is the variation of hardness of Ni-Al_2O_3 thin film composites as a function of the size of Ni particles embedded in Al_2O_3 matrix. For the sake of comparison, we have shown in the figure the hardness data of pure alumina film deposited under identical conditions. It is clear from the figure that the hardness of Ni-alumina composite is significantly higher than that of pure alumina films.

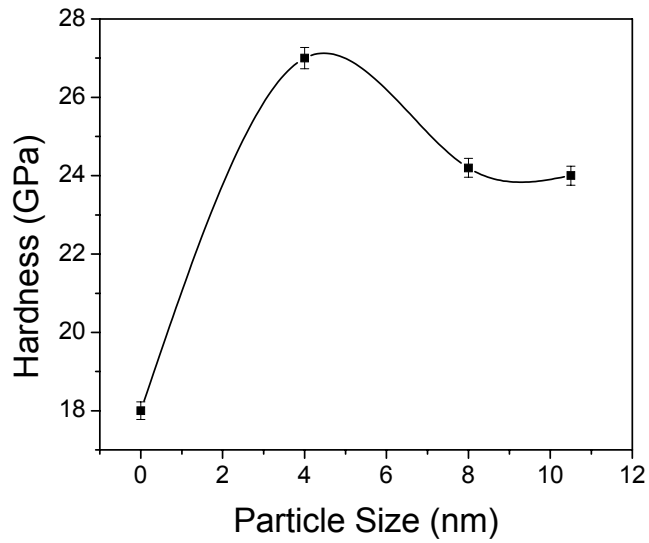

Figure 2. Variation of hardness of Ni-Al_2O_3 thin film composites as a function of the size of Ni particles embedded in Al_2O_3 matrix.

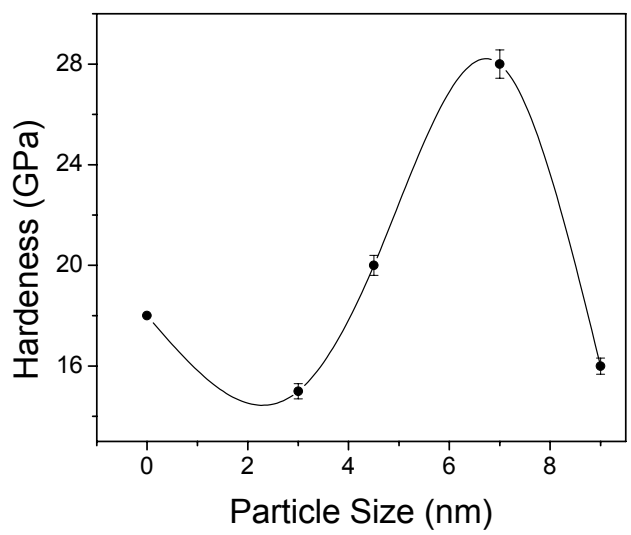

Figure 3. Variation of hardness of Fe-Al_2O_3 thin film composites as a function of the size of Fe particles embedded in Al_2O_3 matrix.

However, a further increase in the particle size of embedded Ni particles resulted in the deterioration of hardness suggesting that there is an optimum size of metal particles, which imparts the composite the highest hardness. A supporting evidence in favor of this suggestion comes from our hardness measurements performed on a different thin film

Copyright © 2002 by ASME

composite system consisted of Fe nanocrystals in alumina thin films. The results obtained are shown in Fig. 3.

According to the results presented in this figure, the hardness of first Fe-Al_2O_3 composite (size of Fe particles 3 nm) is in fact lower than that of pure alumina film. However, the hardness of Fe- Al_2O_3 composite becomes more than that of pure alumina thin film when the size of the embedded Fe nanocrystals increases to 4.5 nm and the hardness reaches a peak at 7 nm, beyond which the hardness of the Fe-Al_2O_3 thin films composite (Fe particle size 9 nm) is again lower than that of pure alumina thin film.

The improvement in values of hardness of Al_2O_3 thin films by embedding metal nanocrystals is related to the evolution of a microstructure which efficiently hinders the manipulation and movement of dislocation and the growth of microcracks, which in turn, is achieved by grain boundary hardening described by Hall-Petch relationship (valid down to a crystallite size of 20-50 nm [19-21]):

$$\sigma_c = \sigma_0 + \frac{k_{gb}}{\sqrt{d}}$$

Here is σ_c the critical fracture stress, d the crystallite size, σ_0 and k_{gb} are constants. With the crystallite size decreasing this limit, the fraction of the material in the grain boundaries increases which leads to a decrease in its strength and hardness due to an increase of grain boundary sliding [22-26]. A simple phenomenological model has been used to describe the softening in terms of an increasing volume fraction of the grain boundary material f_{gb} with the crystallite size decreasing below 1-6 nm [27]:

$$H(f_{gb}) = (1 - f_{gb})H_c + f_{gb}H_{gb},$$

with f_{gb} α $(1/d)$. Due to the flaws present, the hardness of grain boundary materials h_{gb} is smaller than that of the crystallites H_c. Thus the average hardness of the material decreases with d decreasing below 10 nm, an effect commonly known as reverse Hall-Petch effect [28]. Recent computer simulation studies confirm that the reverse Hall-Petch dependence in nanocrystalline materials is due to the grain boundary sliding that occurs due to a large number of small sliding event of atomic plains at the grain boundaries without thermal activation, and therefore will ultimately impose a limit on how strong nanocrystalline metal may become [28-30]. Although many details are still not understood, there is little doubt that grain boundary sliding is the reason for softening in this crystallite size range. Therefore, a further increase of the strength of hardness with decreasing crystallite size can be achieved only if grain boundary sliding is blocked by appropriate design of the material [29-31]. We have tried to achieve this condition by having a uniform distribution of isolated nanocrystals in an amorphous thin film matrix. In such situations, the grain boundaries formed at the interface are very strong and avoid or greatly reduce the grain boundary sliding. We believe that this is what primarily responsible for the realization of higher values of hardness for metal-alumina thin film composites consisted of isolated nanocrystalline metal particles (size below 10 nm) in amorphous matrices.

Shown in Fig. 4 is the cross sectional STEM-Z micrograph of Ni nanocrystallites embedded in alumina matrix. Z-contrast in the STEM provides an incoherent image in which changes in atomic structure and composition across an interface can be interpreted directly without the need for preconceived atomic structure models. This is true provided the incident electron probe is smaller than the lattice spacing (for sample oriented along a major axis) or atomic columns. Since the probe is scanned, the resultant image is a map of the column, scattering power of which in turn depends upon the atomic number, Z^2 of each column. The spatial resolution is limited primarily by the probe size which is 1.2 Å in our field emission instrument.

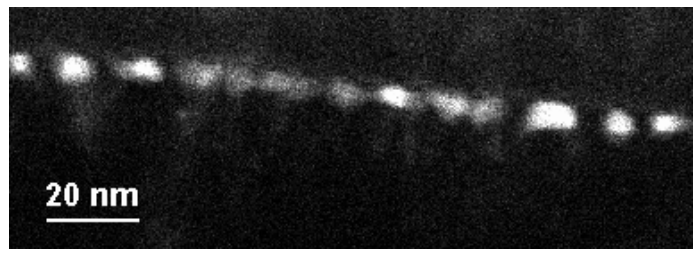

Figure 4. Cross sectional STEM-Z micrograph of Ni nanocrystallites embedded in alumina matrix

The Z-contrast image in the STEM is formed by electron scattered through high angles. The average size of the Ni nanocrystals was determined to be ~5 nm. It is clear from the cross sectional images that the Ni nanoparticles are mostly uniform in size and are well separated from each other. The average intralayer separation between the particles is estimated to be ~2-5 nm. In order to evaluate the crystalline quality of the metal particles and the alumina matrix, a high resolution STEM-Z was recorded (Fig. 5) from a single metal particles and alumina matrix in its immediate vicinity. It is clear from this figure that the Ni nanoparticle is crystalline and the alumina matrix is amorphous in nature. Such a biphase system is formed as both materials are immiscible (i.e., they display thermodynamically driven segregation during deposition) and the cohesive energy at the interface between the both phases is high. The amorphous phase of the matrix can provide high structural flexibility in order to accommodate the coherency strain without forming dangling bonds, voids or other flaw as observed in Fig.5. In this case the nanostructure would be stable and the grain boundary sliding is greatly avoided.

Copyright © 2002 by ASME

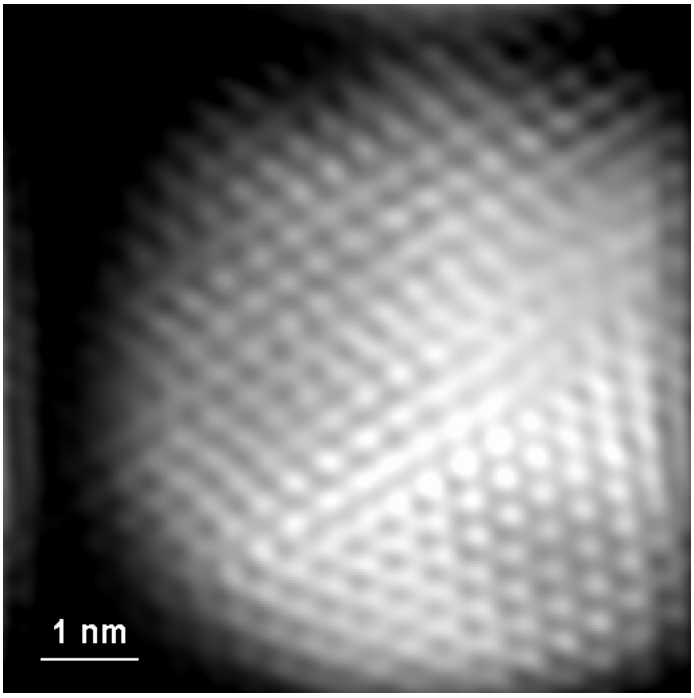

Figure 5. A high resolution STEM-Z recorded from a single Ni particles and alumina matrix in its immediate vicinity.

The improvement in the values of hardness of Al_2O_3 by embedding Ni and Fe nanoparticles may also be explained using the Koehler concept of mulitlayers for the design of strong solids [32]. According to his concept, under applied stress a dislocation which would form in softer layer (metal in the present study), would move toward the metal-ceramic interface, elastic strain in the second layer (alumina in the present study) with the higher elastic modulus would cause a repulsing force that would hinder the dislocation from crossing that interface. Therefore, the hardness of Ni-Al_2O_3 and Fe-Al_2O_3 thin film composites, which are essentially multilayered structures costing of continuous layer of alumina thin films and discontinuous film of metals, is much larger than expected from the rule of mixture.

CONCLUSIONS

In summary, we have fabricated thin films composite materials consisting of metallic nanocrystals embedded in an insulator host with significantly improved mechanical properties. The improvement in the hardness of Al_2O_3 thin films by embedding metal nanocrystals is related to the evolution of a microstructure, which impedes the manipulation and movement of dislocation and the growth of microcracks. The impedance in grain boundary movement is brought about by grain boundary hardening due to formation of well-separated metallic nanocrystallites in amorphous matrices.

References

[1] Stamm, C., Marty, F., Vaterlaus,A., Weich, V, Egger,S., Maier, U., Ramsperger,U., Fuhrmann, H., and Pescia, D., Science, 1998, Vol. 282, pp. 449-451.

[2] Lu, L., Sui, M.L., and Lu, L., Science, 2000, Vol. 287, pp. 1463-1467.

[3] Timp, G., Nanotechnology, 1999, Springer, New York.

[4] Kumar, D., Narayan, J., Kvit,A.V., Sharma, A.K., Sankar,J., Journal of Magnetism and Magnetic Materials, 2001, Vol. 232, 161-167.

[5] Kumar, D., Zhou,H, Nath, T.K., Kvit, A.V., and Narayan, J, Applied Physics Letters, 2001, Vol. 79, pp. 2817-2819.

[6] Prinz, G.A., Science, 1998, Vol. 282, pp. 1660-1662.

[7] Mehn, M., Punadjela, K., Bucher,J., Roussseausx, F., Decanini,D., Bartenlian,B., and Chappert, C., Science, 1996, Vol. 272, pp. 1782-1785.

[8] Katiyar, P., Kumar, D., Nath, T.K., Kvit, A.V., J. Narayan, S. Chattopadhyay, S., Gilmore, W.M., Coleman, S., Lee, C.B., Sankar, J., and Singh, R.K., Applied Physics Letters, 2001, Vol. 79, pp. 1327-1329.

[9] Ballesteros, J.M., Serna, R., Solis, J., Afonso, C,N., Petford-Long, A.K., Osborne, D.H., and Haglund, Jr., R.F., Applied Physics Letters, 1997, Vol. **71**, 2445-2447.

[10] Hirono, S., Umemura, S., Tomita, M., and, Kaneko, R., Applied Physics Letters, 2002, Vol. 80, pp. 425-428.

[11] Veprek, S., Journal of Vacuum Science and Technology A, 1999, Vol. 17, pp. 2401-2404.

[12] Cselle, T., and Barimani, A., Surface Coating and Technology, 1995, Vol. 76-77, pp. 712-716.

[13] Rodeghiero, E.D., Tse, O.K., Chisaki,J., Giannelis, E.P., Materials Science and Engineering A, 1995, Vol. 195, pp. 151-161.

[14] Sekino,T., Nakajima, T., Ueda, S., and Niihara, K., Journal of American Ceramic Society, 1997, Vol. 80, pp. 1139.

[15] Lu, K., Wang, T., and Wei, W.D., Journal of Applied Physics, 1991, Vol. 69, pp. 522-527.

[16] De, G., Tapfer, L., Catalano, M., Battaglin, G., Caccavale, F., Gonella, F., Mazzoldi, P., and Haglund, Jr., R.F., Applied Physics Letters, Vol. 68, pp. 3820.

[17] Liao, H.B., Xiao, R.F., Fu, J.S., Yu, P., Wong, G.K.L., and Sheng, P., Applied Physics Letters, 1997, Vol. **70**, pp. 1-3.

[18] Mazzoldi, P., Arnold,G.W., Battaglin,G., Bertoncello,R., and Gonella,F., Phys. Res. B, 1994, Vol**. 91**, pp. 478-483.

Copyright © 2002 by ASME

[19] Hertzberg, R.W., Deformation and Fracture Mechanics of Enginnering materials, 1989, 3rd ed. , Wiley, New York.

[20] Hall, E.O., Proceedings of Physical Society London, 1951, Vol. B64, pp. 747-758.

[21] Petch, N.J., J. Iron Steel Instruments, London, 1953, Vol. 174, pp. 25-38.

[22] Siegel, R.W., and Fougere, G.E., Nanostructured Materials, 1995, Vol. **6**, pp. 205-209.

[23] Siegel, R.W., and Fougere, R.W., Nanostruc. Mater **6**, 205 (1995).

[24] Hahn, H., and Padmanabhan, K.A., Philosophical Magazine B, 1997, Vol. 76, pp. 559-568.

[25] Yip, S., Nature, London, 1998, Vol. 391, pp. 532-535.

[26] Schiotz, J., Tolla, D., and Jacobsen,K.W., Nature (London), 1998, Vol. 391, pp.561-563.

[27] Carsley, J.E., Ning, J., Milligan, W.W., Hackney, S.A. and Aifantis, E.C., Nanostruc. Mater. **5**, 441 (1995).

[28] Chokshi, A.H., Rosen, A., Karch, J., and Gleiter, H., Scr. Metall. **23**, 1679 (1989).

[29] Nieman, G.W., Weertman, J.R., and Siegel,R.W., Journal of Materials Research , 1991, Vol. 6, pp. 1012.

[30] Sanders,P.G., Youngdahl,C.J., and Weertman, J.R., Materials Science and Engineering A, 1997, Vol. 234, pp. 77-83.

[31] Youngdahl, C.J., Sanders, P.G., Eastman, J.A. and Weertman, J.R., Scr. Mater. **37**, 809 (1997).

[32] Koehler, J.S., Phys. B, 1970, Vol. 2, pp. 547-552.

Copyright © 2002 by ASME